DFT Study of Lewis Base Interactions with the MgCl2 Surface in the Ziegler−Natta Catalytic System: Expanding the Role of the Donors

ARTICLE *in* THE JOURNAL OF PHYSICAL CHEMISTRY C · SEPTEMBER 2010

Impact Factor: 4.77 · DOI: 10.1021/jp106673b

4 AUTHORS:

Kumar Vanka
CSIR - National Chemical Laboratory, Pune
61 PUBLICATIONS **824** CITATIONS
SEE PROFILE

Divya Iyer
Texas Tech University
2 PUBLICATIONS **19** CITATIONS
SEE PROFILE

Gurmeet Singh
IndianOil-R&D
22 PUBLICATIONS **220** CITATIONS
SEE PROFILE

Virendra K. Gupta
Reliance Industries Limited
48 PUBLICATIONS **316** CITATIONS
SEE PROFILE

DFT Study of Lewis Base Interactions with the $MgCl_2$ Surface in the Ziegler−Natta Catalytic System: Expanding the Role of the Donors

Kumar Vanka,*,† Gurmeet Singh,‡ Divya Iyer,† and Virendra K. Gupta*,‡

Physical Chemistry Division, National Chemical Laboratory, Dr. Homi Bhabha Road, Pashan, Pune, Maharashtra-411 008, India, and Reliance Technology Group - Hazira, Reliance Industries Ltd., Hazira Complex, Surat, Gujarat-394 510, India

Received: July 18, 2010

We present a computational study, using density functional theory, of the role of internal and external donors in supported heterogeneous Ziegler−Natta polymerization catalyst systems. The focus of the investigation is the ability of the donors to stabilize the $MgCl_2$ support through the zip mode of coordination. Phthalates and alkoxy benzoates have been considered as representative internal and external donors, respectively. Models for the α (ccp) and the β (hcp) phases of the (110) $MgCl_2$ lateral cut have been considered. Studies were first done with a "Fully Fixed Model", where the atoms in the $MgCl_2$ lateral cuts were kept fixed. The studies indicated that the phthalate donors would preferentially stabilize the α phase of $MgCl_2$, while the alkoxy benzoate donors would stabilize the β phase more, corroborating experimental results. A comparison of the zip coordination mode with other modes of coordination (mono, chelate, and bridge) indicates that it would be preferred over the mono and chelate coordination modes and be competitive with the bridge coordination mode. The validity of the Fully Fixed Model was then tested by doing calculations with the Partially Relaxed (some of the magnesium and chlorine atoms unfixed) and the Fully Relaxed (all atoms free) Models. The results from the latter two models corrected some of the discrepancies that had been observed for the Fully Fixed Model in comparison to previous experimental and computational investigations but were in general agreement with the Fully Fixed Model, indicating that the overall conclusions drawn with the earlier model are correct. Insertion studies done on an octahedrally coordinated titanium site flanked by two zip-coordinated phthalate donor molecules indicated that the zip-coordinating donors can confer exceptional regioselectivity to the titanium center. A list of potential donors that could serve as external donors, with di-iso-butyl phthalate (DIBP) as the internal donor, was investigated, and it was found that 1,3-diethers would serve as the best external donors to DIBP.

Introduction

Ziegler−Natta catalysis has played a dominant role in industrial polyolefin production[1−4] by providing high productivity and stereoregularity,[4−13] thus becoming one of the most important industrial processes. The major transformation in Ziegler−Natta catalysis can be attributed to the introduction of the $MgCl_2$ matrix, resulting in better morphology control and multifold enhancement in the productivity.

The $MgCl_2$ matrix, with a crystal structure similar to $TiCl_3$, is composed of irregularly stacked Cl−Mg−Cl sandwich-like monolayers characterized by the presence of lateral cuts that are occupied by magnesium cations with unsaturated coordination.[14−18] The lateral cuts have been designated as (100) or (104) for five-coordinated and (110) for four-coordinated magnesium cations for the α-$MgCl_2$ phase, in comparison to six-coordinated magnesium cations in the bulk, making these sites Lewis acidic.[19−22] In addition to α-$MgCl_2$ (cubic close packed (ccp) structure), β-phase $MgCl_2$ (hexagonal close packed (hcp) structure) and the disordered δ-phase of $MgCl_2$ are also known to exist in the $MgCl_2$ matrix in Ziegler−Natta catalysts.[23−28] Figure 1 shows the structures of crystalline α and β $MgCl_2$ phases, with identical triple layer structures.

Successive generations of the Ziegler−Natta catalysts have evolved into a multicomponent system comprising, in addition to $TiCl_4$, $MgCl_2$, and the alkylating agent AlR_3 (R = Et being the most employed), (i) internal donors, aromatic esters (benzoates and phthalates, in particular), and recently, succinates and 1,3-diethers, and (ii) external donors, alkoxy benzoates and alkoxy silanes. The commonly accepted roles[29−32] of the internal and external donors during the polymerization appear to be to bind to the (110) lateral cuts of $MgCl_2$ and thereby provide (i) stability to the more acidic, four-coordinate (110) $MgCl_2$ surfaces and (ii) stereoregulating control to active titanium catalysts adjacently bound to the same (110) $MgCl_2$ surface. Therefore, the manner in which the donor can bind to the $MgCl_2$ surface is a question of significance. It is generally believed[35] that there are four ways in which donors containing two oxygen atoms that can bind to $MgCl_2$ can coordinate to the support: (i) the coordination of one oxygen of a donor molecule to one magnesium atom, the "monocoordination" mode, (ii) the coordination of both oxygen atoms of the donor molecule to the same magnesium atom, the "chelate" coordination mode, (iii) the coordination of both oxygens of the donor molecule to two magnesium atoms on the same layer, the "bridge coordination" mode, and (iv) the coordination of both oxygens of the donor molecule to two magnesium atoms on different, adjacent $MgCl_2$ layers, the "zip"-coordination mode, which Correa et al.[40] have shown to be a viable binding option for the donor

* To whom correspondence should be addressed. E-mail: k.vanka@ncl.res.in; virendrakumar_gupta@ril.com.
† National Chemical Laboratory.
‡ Reliance Industries Ltd.

10.1021/jp106673b
Published on Web 08/30/2010

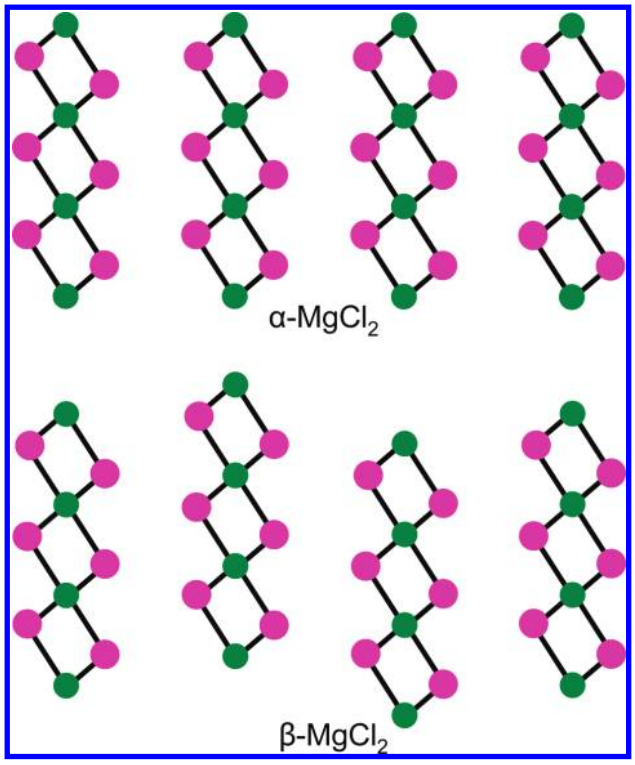

Figure 1. α and β phases of $MgCl_2$ with identical triple layer structures.

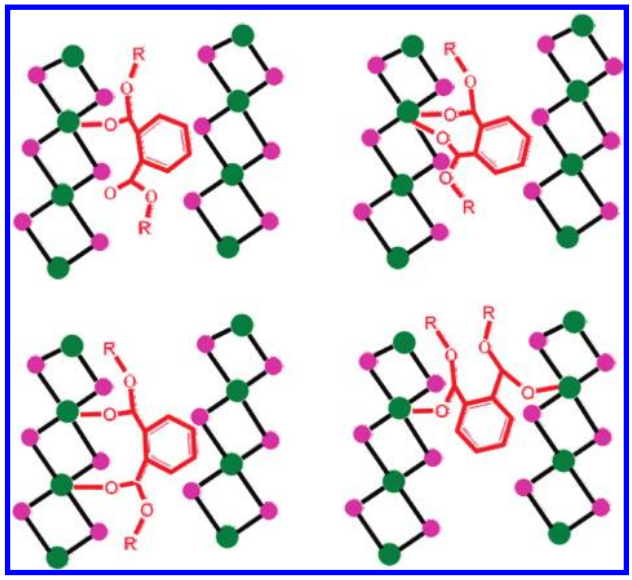

Figure 2. Four possible modes of coordination of a donor molecule (in this case, a phthalate) to $MgCl_2$ layers; clockwise from top left: the monocoordination, chelate coordination, zip coordination, and bridge coordination modes.

(the four modes of coordination of the donor to the $MgCl_2$ surface are shown in Figure 2, with a phthalate as the donor).

Computational work in this field has been used to bolster the experimental findings, as well as provide an independent route to investigating the $MgCl_2/TiCl_4$/donor(s) system. The work has focused on (i) purely molecular mechanics approaches,[33] (ii) semiempirical approaches[34] and quantum mechanical approaches, such as an embedded QMMM method,[35−37] full QM calculations[38] and periodic density functional theory calculations.[20,30,39] Molecular dynamics simulations using periodic density functional theory calculations have been conducted by Boero, Parrinello, and co-workers to look at propene polymerization[30] and to look at different active surfaces and catalytic sites to gain a better understanding of the coordination of the titanium species on different active surfaces and sites in the $MgCl_2/TiCl_4$ surface. More recently, Busico and co-workers have used periodic DFT calculations in conjunction with high resolution magic angle spinning (HR-MAS) ^{1}H NMR spectroscopy to look at different $MgCl_2$ surfaces and concluded that the dominant lateral surface for the $MgCl_2$ crystals was (104).[20] Periodic density functional theory (DFT) has been used by Zakharov's group[39] to study the coordination of carbon monoxide on different models of the $MgCl_2$ surface, to compare to experimental IR spectra, obtained from DRIFT spectroscopy. The Ziegler group has used the embedded QMMM method to look at the binding and polymerization termination reactions of ethylene to different active sites in the $TiCl_4/MgCl_2$ catalyst system,[35] to study the effects of an external base (tetrahydrofuran, THF) on ethylene polymerization properties[36] and the copolymerization of ethylene and propylene on the $TiCl_3$-based slope site.[37] Flisak[36b] has studied the influence of the tetrahydrofurfuryloxide ligand on catalyst selectivity. Correa et al.,[40] mentioned in reference to the zip coordination mode earlier, have conducted an extensive examination on the possible role of the internal donors, diethers, alkoxysilanes, phthalates, and succinates, on modulating the behavior of the $MgCl_2/TiCl_4$ catalyst system, and also studied the stereo- and regioselective behavior of possible titanium species with and without two succinate molecules coordinated within the proximity of the titanium atom.

The computational studies have provided valuable insights into the $MgCl_2/TiCl_4$/donor(s) system, but, given the importance of understanding the donor−$MgCl_2$ interaction, there is still considerable scope for investigation. For one, the studies to date have focused only on the coordination of the donor on a single layer of $MgCl_2$, and only the α $MgCl_2$ phase has been considered, even though there is no theoretical proof that the donors prefer the α phase over the β. Also, it has been noted experimentally[41−44] that the alkoxy benzoate external donors work well when the internal donor employed is ethyl benzoate, but are far less effective when phthalates are used as the internal donors, but no explanation for this has so far been put forth. Moreover, different phases of $MgCl_2$ appear to be stabilized in the presence of different donors: the α phase is seen to be the more prevalent when phthalates are used as the internal donors, while with ethyl benzoate as the internal donor, it is the β phase of $MgCl_2$ that is the more prevalent.[45] It is possible that the donor, through the zip coordination mode, may be playing an important role in preferentially stabilizing the α or the β lateral cut of $MgCl_2$ and thereby leading to the observed experimental results.

The current computational investigation aims to address these issues. The objective is to develop and expand on the current understanding of the role of internal and external donors by focusing on the relative stabilities of the complexes formed by internal and external donors when zip-coordinated to α and β phases of $MgCl_2$. To this end, two donor families, the phthalate internal donors, di-isobutyl phthalate (henceforth referred to as DIBP) and diethyl phthalate (DEP), and the alkoxy benzoate external donors, *p*-ethoxy, *p*-isopropoxy, and *p*-*tert*-butoxy benzoates, have been considered in this study. It is also important to note that, with the donor coordinated in the zip coordination mode, one can consider different interlayer distances (shown as "*x*" in Figure 3) between adjacent α or β $MgCl_2$ layers. This is pertinent because peak broadening for

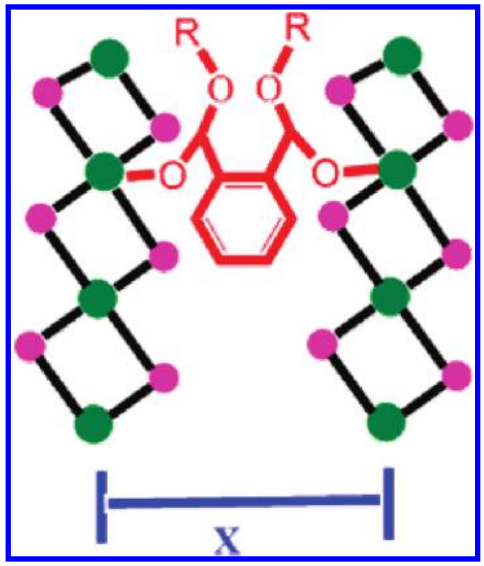

Figure 3. Interlayer distance (represented by "*x*") between adjacent $MgCl_2$ layers (α or *β*) zip coordinated by a donor can vary.

the peak corresponding to the separation of adjacent $MgCl_2$ triple layers toward lower 2θ values has been observed in the XRD spectra when the donor is coordinated to the $MgCl_2$ surface,[45] which indicates the possibility of the donor stabilizing the triple layers of $MgCl_2$ at different "*x*" values. A representative sample of four values for *x*, 5.9, 6.3, 6.6, and 7.9 Å, has been considered for the α and *β* phases of $MgCl_2$. Moreover, the mono, chelate, and bridge coordination modes of binding have also been considered for the DIBP donor. Also, in addition to the (110) lateral cut, the coordination of DIBP to the (104) lateral cut (for α-$MgCl_2$) and the (011) lateral cut (for α-$MgCl_2$) have been considered for purposes of comparison. All of these investigations have been undertaken with a Fully Fixed $MgCl_2$ Model, where the magnesium and chlorine atoms in all the structures investigated were kept fixed. The validity of this model has then been further tested by doing studies with Partially and Fully Relaxed models (described in the Computational Details) to represent the α and *β* $MgCl_2$ lateral cuts.

After having tested and established the best model for investigating the zip coordination, the effect of the zip-coordinating donors on the regio- and stereoselectivity of the chiral, octahedral titanium center has been studied by flanking a titanium center by two zip-coordinated DIBP donor molecules and investigating the primary and secondary insertion of propylene.

Finally, a comparative study has been conducted to determine the relative binding affinities of different donors that could serve as potential replacement for a DIBP molecule should it be removed from the $MgCl_2$ surface, that is, act as a potential external donor when DIBP is the internal donor.

Computational Details

Calculations with DFT. All the calculations were carried out using density functional theory using the Turbomole suite of programs.[46−49] Geometry optimizations were performed using the Perdew, Burke, and Erzenhof density functional.[50,51] The electronic configuration of the atoms was described by a triple-ζ basis set augmented by a polarization function (TURBOMOLE basis set TZVP).[52] The resolution of identity (RI)[53] along with the multipole accelerated resolution of identity (marij)[54] approximations were employed for an accurate and efficient treatment of the electronic Coulomb term in the density functional calculations. Keeping in mind that relative ΔE values are discussed in the manuscript, we estimate the reliability and accuracy of the calculated ΔE values to be within ±0.5 kcal/mol.

$MgCl_2$/Donor Interactions. The geometries of the adsorbed donor molecules have been fully optimized in all cases. α and *β* phases have been considered for the $MgCl_2$ clusters. The (110) and (104) lateral cuts have been considered for the α phase of $MgCl_2$, representing four and five coordinate magnesium atoms, respectively. For the *β* phase, the (110) and the (011) lateral cuts have been considered to represent the same. The 3-D models of α and *β* $MgCl_2$ were generated using the Diamond Software,[55] with crystallographic parameters taken from literature reported earlier.[25] To change the interlayer distance between the α and *β* phases, two layers of the required $MgCl_2$ lateral cut were created using the Mercury software[56] and then the coordinates of one layer were fixed and the second layer was translated to the required distance away from the first layer.

Three different models for $MgCl_2$ have been considered in this study. First, calculations were done keeping all the atoms in the $MgCl_2$ lateral cuts fixed: the "Fully Fixed" model. As has been noted in several previous computational studies, this model, based on the simplifying assumption that the atoms on the surface are close in structure to the bulk, can be expected to preserve the trends in the relative coordination energies.[40,57−61]

Because the scope and the objective of the present work is to compare and contrast different donors, as well as compare the binding for the same donor to the same lateral cut at different interlayer distances, we believe that this is a reliable approach. Nevertheless, calculations have also been done with a "Partially Relaxed" model, where the surface magnesium and chlorine atoms were kept unfixed. This was specifically done to study the zip coordination of the donor DIBP on to the lateral cuts of α and *β* $MgCl_2$ layers at different interlayer distances so as to address some discrepancies between the current calculations with the Fully Fixed Model and previous experimental results (discussed below in Results and Discussion). Calculations have been done to validate both the Fully Fixed and the Partially Relaxed Models with periodic DFT calculations. This has been done by calculating the binding energy of the species (i) $TiCl_4$ and (ii) ethyl benzoate to the $MgCl_2$ support modeled as Fully Fixed and Partially Relaxed and comparing the results with the periodic DFT calculations done by Taniike et al.[62] The results are tabulated and provided in the Supporting Information.

Finally, a "Fully Relaxed" model, where all the magnesium and chlorine atoms in the α and *β* lateral cuts were allowed to move, was also studied. This was done to calculate the free energies of binding ($-\Delta G$), calculated at 298.15 K, and also to determine the (>C═O) stretching frequencies, to compare to (>C═O) stretching frequencies obtained in experimental studies. A scaling factor of 0.9 is employed in Turbomole to scale down the obtained vibrational frequencies.

The donor adsorption energy, represented as ΔE in the tables, is calculated according to

$$\Delta E = E_{Mg/D} - E^0_{Mg} - E^0_D \quad (1)$$

where $E_{Mg/D}$ is the energy of the complex formed by the donor coordinating to the $MgCl_2$ cluster, while E^0_{Mg} and E^0_D are the total energies of the $MgCl_2$ cluster and of the donor molecule, respectively.

Likewise, the donor adsorption free energy, represented as ΔG in Table 4, is calculated according to

$$\Delta G = G_{Mg/D} - G^0_{Mg} - G^0_D \quad (2)$$

where $G_{Mg/D}$ is the energy of the complex formed by the donor coordinating to the $MgCl_2$ cluster, while G^0_{Mg} and G^0_D are the total energies of the $MgCl_2$ cluster and of the donor molecule, respectively.

Insertion Studies. With regard to the insertion studies, unrestricted calculations were done because of the presence of the Ti(III) active species. Because of the size of the systems considered, transition state searches for primary and secondary propene insertion into the Ti−*i*Bu bond were approximated through a linear scan of the potential energy surface in the region 2.05−2.45 Å of the new forming C−C bond with a step of 0.05 Å. All other degrees of freedom were optimized. This choice is based on the fact that the forming C−C bond in transition states for insertion of ethene or propene into Ti-alkyl bonds is almost invariably calculated to be in this range.[9,35−37,66] In each case, the geometry highest in energy along the potential energy scan was considered to be a reasonable approximation to the real transition state. A similar approach was used before, most notably by Correa et al., for doing a similarly difficult search for a similarly coordinated octahedral Ti(III) active site,[40] as well as by Ziegler and co-workers in the comparatively difficult case of acrylates polymerization.[67]

Results and Discussion

(A) The Fully Fixed $MgCl_2$ Model. The Fully Fixed Model (described in Computational Details) is considered first. Before discussing the zip coordination mode of donor binding, it is noted here that the uncoordinated α $MgCl_2$ layers were found to be more stable than the β, by 4.8 kcal/mol. This indicates that there will be a higher proportion of α $MgCl_2$ present in the system, before donor coordination. The following sections discuss how these proportions might be changed by the way the donor can stabilize the α and β $MgCl_2$ layers, through the zip coordination mode.

Zip Coordination for the 110 Lateral Cut: The Phthalate Donors. The zip coordination mode is considered first for the two phthalate donors DIBP (di-isobutyl phthalate) and DEP (diethyl phthalate). Gathered in Table 1 are the values for the zip coordination (ΔE in kcal/mol) of the DIBP donor to the α and β (110) $MgCl_2$ layers, at four separate interlayer distances: 5.9, 6.3, 6.6, and 7.9 Å. This range: 5.9−7.9 Å was chosen because this was the range of interlayer distance for which Singh et al.[45] observed WAXD peaks in their experimental investigations of $MgCl_2$/$TiCl_4$/DIBP systems.

The values in Table 1 indicate that the binding energies ($-\Delta E$) of DIBP are greater for α $MgCl_2$ layers than for β, for the entire range studied. The explanation for this lies in the greater steric crowding in zip-coordinated β phase $MgCl_2$ in comparison to the α, as illustrated in Figure 4. To take a specific example, when the interlayer distance is 5.9 Å, the average distance of the six carbons of the phenyl ring from the two chlorine atoms shown in Figure 4 is 4.6 Å for the α $MgCl_2$ case and 4.1 Å for the β $MgCl_2$ case. The other reason is that the phthalate molecule has to distort itself to a greater extent from its free, fully relaxed state to coordinate to the magnesium atoms in β $MgCl_2$. This was seen when single point calculations were done to determine the energy of just the distorted, zip-coordinated DIBP structure taken from the α and β cases, with the 5.9 Å case taken as an example. It was found that the β case DIBP structure was 3.1 kcal/mol higher in energy than the corresponding structure in the α case.

TABLE 1: Values of ΔE Obtained for the Zip Coordination of the Internal Donor Di-isobutyl Phthalate and Diethyl Phthalate onto the (110) α and β Layers of $MgCl_2$

	ΔE (kcal/mol)	
distance (Å) between layers	α	β
Di-isobutyl Phthalate		
5.9	−39.1	−33.4
6.3	−33.0	−29.4
6.6	−33.3	−20.0
7.9	−25.3	−23.3
Diethyl Phthalate		
5.9	−37.7	−32.7
6.6	−31.2	−21.2

This result provides an explanation for experimental observations[45] finding greater concentrations of α $MgCl_2$ over β when DIBP was used as an internal donor. By coordinating through the zip coordination mode, DIBP would stabilize the α phase of $MgCl_2$ more than the β.

It should be noted here that disfavoring entropic effects, not reflected in the ΔE values, could reduce the ability of the phthalate donor to stabilize α $MgCl_2$. This issue is addressed in Section C - when discussing the Fully Relaxed Model.

It should also be noted that there is a distinct trend vis-a-vis the interlayer distance and the binding energy: as the distance between the adjacent $MgCl_2$ layers is increased, the binding energy is seen to decrease. When the interlayer distance is 7.9 Å, the value of ΔE was seen to drop off to −25.3 and −23.3 kcal/mol for the α and β cases respectively. This is because the DIBP donor no longer zip coordinates to the α and β layers when the interlayer distance has increased to 7.9 Å, but is only monocoordinated to one of the two $MgCl_2$ layers. As will be discussed in Section B later, we have addressed this issue by investigating the zip coordination mode with the surface magnesium and chlorine atoms of the lateral cuts in the two adjacent $MgCl_2$ layers relaxed, the "Partially Relaxed" model (see section B).

Calculations have also been done with DEP as the internal donor, and the results for the set of calculations {the binding energy ($-\Delta E$) to α and β $MgCl_2$} are shown in Table 1. The binding energies are seen to follow the same trend as they had done for the DIBP case but are less exothermic than the corresponding DIBP numbers by about 2.0 kcal/mol. This is understandable because the iso-butyl group is more electron donating than the diethyl group, and the implication of this result is that DEP would not do as good a job at stabilizing the $MgCl_2$ donors through the zip coordination as DIBP.

Alkoxy Benzoate External Donors. As mentioned in the Introduction, we have also investigated the zip coordination for

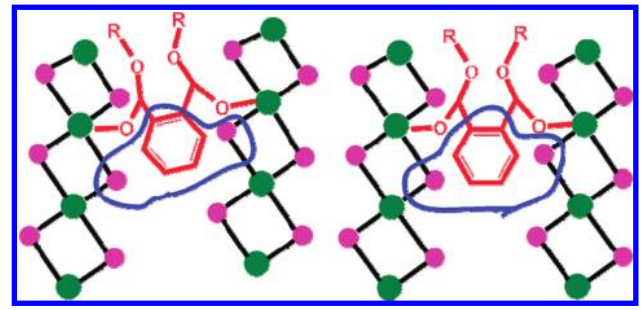

Figure 4. Coordination of the phthalate donor when zip-coordinated to the α and β lateral cuts of $MgCl_2$: there is more steric interaction of the phenyl ring of the phthalate with chlorine atoms in the β $MgCl_2$ case (structure on the right).

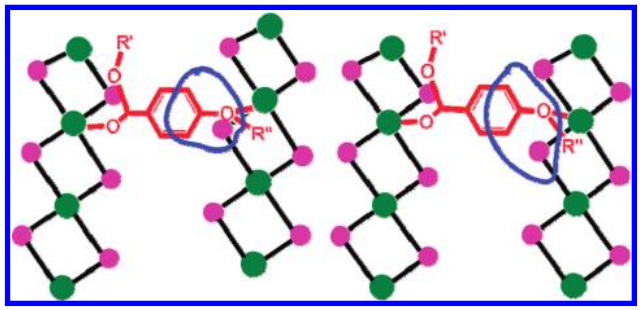

Figure 5. Coordination of the alkoxy benzoate donor when zip coordinated to the α and β lateral cuts of $MgCl_2$: there is more steric interaction of the phenyl ring of the phthalate with chlorine atoms in the α $MgCl_2$ case (structure on the left).

TABLE 2: Values of Δ*E* Obtained for the Zip Coordination of the External Donor *p*-Iso-propoxy Ethyl Benzoate, *p*-Ethoxy Ethyl Benzoate, and *p-tert*-Butyl Ethyl Benzoate on to the (110) α and *β* Layers of $MgCl_2$

	Δ*E* (kcal/mol)					
	p-iso-propoxy ethyl benzoate		*p*-ethoxy ethyl benzoate		*p-tert*-butyl ethyl benzoate	
distance (Å) between layers	α	*β*	α	*β*	α	*β*
5.9	−32.3	−28.7	−29.7	−26.3	−34.5	−31.7
6.3	−29.2	−36.6	−30.1	−35.9	−34.3	−40.2
6.6	−27.6	−37.8	−30.7	−37.3	−34.3	−41.7
7.9	−24.1	−34.1				

the alkoxy benzoate external donors: *p*-isopropoxy, *p*-ethoxy, and *p-tert*-butoxy benzoate. Figure 5 shows the optimized structure for the zip-coordinated external donor *p*-isopropoxy benzoate on to two (110) *β* layers of $MgCl_2$ separated by 5.9 Å. In Table 2 are the values of Δ*E* for the zip coordination for the three esters.

From the tabulated results, it is noted that, for the 5.9 Å case, the coordination of α $MgCl_2$ is preferred over the *β*, for all the three alkoxy benzoates studied. To understand this result, it should first be noted that the distance between the two donor binding magnesium atoms is always shorter in the *β* phase $MgCl_2$ because of the relative orientation of the adjacent α and *β* $MgCl_2$ layers (see Figure 1). Now, for the 5.9 Å case, the phenyl ring in the alkoxy benzoate, which prefers to be flat, has to distort more in *β* $MgCl_2$ than in α, because of the reduced distance between the *β* $MgCl_2$ layers and, hence, the preferred coordination to α $MgCl_2$ over *β*.

For the remaining cases, 6.3, 6.6, and 7.9 Å, the distance between the coordinating magnesium atoms is sufficient to accommodate the phenyl ring without necessitating its distortion, for both the α and *β* $MgCl_2$ cases. It is seen, from the Δ*E* values in Table 2, that for these three interlayer distances, the alkoxy benzoate always prefers to coordinate to *β* $MgCl_2$ over α $MgCl_2$. The reason for this is illustrated in Figure 5; there is greater steric crowding in the α cases for the zip-coordinated alkoxy benzoate complexes in comparison to the *β*. When the interlayer distance is 6.3 Å, for instance, the distance between the *ortho*-carbon in the phenyl ring of the alkoxy benzoate and the chlorine atom inside the blue circle in Figure 5, is 2.97 Å for the α $MgCl_2$ case and 3.25 Å for the *β* $MgCl_2$ case. The greater steric crowding for the α $MgCl_2$ case forces the ether oxygen to bind more weakly to the magnesium atom: the O−Mg distance is 2.37 Å, in comparison to the value of 2.14 Å in the corresponding α $MgCl_2$ complex. Hence, the greater stability of the zip-coordinated alkoxy benzoate *β* $MgCl_2$ complexes over the corresponding α cases.

This interesting result that the alkoxy benzoate would stabilize the *β* $MgCl_2$ phase over the α is exactly the opposite to what had been observed for the phthalate donors, discussed earlier, where the donor preferred to bind to the α $MgCl_2$ layers. This may be the explanation for the experimental observation that has been mentioned earlier in the Introduction, that the alkoxy benzoate donor is much more effective as an external donor when the internal donor is ethyl benzoate (which has only one coordinating oxygen and so cannot zip-coordinate to stabilize α or *β* phase $MgCl_2$) and not a phthalate.[45] The explanation is as follows: with a phthalate as donor, α phase $MgCl_2$ will be present in greater concentration in the Ziegler−Natta system, due to the preferential, stabilizing zip coordinating effect of the phthalate donors, discussed above. Now, should the phthalate be stripped off the $MgCl_2$ by other species present in the system, such as $AlEt_3$, an external donor like alkoxy benzoate will not be an effective substitute for the phthalate. This is because the alkoxy benzoate zip coordinates much better with *β* phase $MgCl_2$ than with α. Hence, such an internal donor external donor combination would not be very effective, corroborating experimental observations.

For the values in the Table 2, it is also noted that the binding energy (−Δ*E*) increases as we increase the substitution on the ether group: from ethyl to iso-propyl to tertiary-butyl. Again, this is consistent with the trend that had been observed for the phthalate cases: the more electron donating the substituent, the better the binding of the donor.

Other Modes of Coordination. The arguments made in the previous section for explaining experimental observations on the basis of the internal and external donors coordinating to $MgCl_2$ through the zip coordination mode implicitly assume that the zip coordination mode is the preferred mode of coordination of the donors with the $MgCl_2$ lateral cuts. It is, however, important to evaluate the other three modes of coordination of the donor, the monocoordination, chelate coordination, and bridge coordination modes (see Figure 2), to ascertain the extent to which they can compete with the zip coordination mode. This was investigated and is discussed in this section, with DIBP being employed as the donor.

Monocoordination. As in the case of the zip coordination mode, three different interlayer distances were considered for the α and *β* phases of (110) $MgCl_2$, leading to six optimized structures. The six binding energies obtained were all found to lie in the range −20.0 to −25.0 kcal/mol. This indicates that, in the case of DIBP, the monocoordination mode of binding is less preferred in comparison to the zip coordination mode to the (110) $MgCl_2$ surface. While this was the hoped for result, it is noted here that calculations with a Fully Relaxed Model, discussed later, show that the Fully Fixed Model underestimates the binding of the donor to the $MgCl_2$ surface.

Chelate Coordination. As discussed in the Introduction, the chelate coordination mode is the binding of two oxygens of the donor (DIBP, in our case) to the same magnesium atom (see Figure 2). This coordination mode was investigated for the α $MgCl_2$ case, with 5.9 Å as the interlayer distance. As shown in Figure 6, the optimized structure loses the chelate coordination and ends up being monocoordinated to the $MgCl_2$ surface. This appears to indicate that the chelate coordination mode is not favored for the phthalate donors. However, chelate coordination for a phthalate on the (110) $MgCl_2$ surface has been reported in the past by Correa et al.[40] Therefore, the reason the chelate coordination is not observed here could also be attributed to a limitation of the Fully Fixed Model. This is investigated further later in section B.

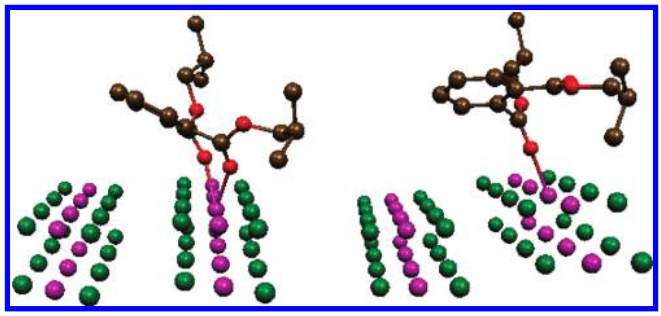

Figure 6. Input structure (left) and final, optimized geometry (right) for the chelate coordination of the di-isobutyl phthalate donor to the same magnesium atom on a layer of α $MgCl_2$ (110) (the distance between the layers is 5.9 Å), for the purpose of clarity hydrogens are not shown.

It is noted here that the chelate coordination mode would be impossible in the case of the alkoxy benzoate donors because of the large distance between the two coordinating oxygens in the ester molecule.

Bridge Coordination. The bridge coordination, discussed in the Introduction, is the coordination of two oxygens of the donor to adjacent magnesium atoms on the same $MgCl_2$ lateral cut (see Figure 2). The binding energy ($-\Delta E$) for the bridge coordination was found to be 40.1 kcal/mol, which is comparable to the binding energy (39.1 kcal/mol) observed for the zip coordination mode. This indicates that the bridge coordination, along with the zip coordination mode, is also a viable option for the DIBP donor and would possibly even be slightly more favored than the zip coordination mode. The influence of entropic effects on this mode of binding is further discussed in section C.

Coordination to Other Lateral Cuts. The focus of the work discussed here is the coordination of the phthalate and the ester donors onto (110) $MgCl_2$ lateral cuts, but we have also looked at one representative case of the donor binding to other $MgCl_2$ lateral cuts, (104) and (011), which are commonly accepted to also be formed during the Ziegler−Natta polymerization process. The donor chosen was DIBP, and the zip coordination mode was considered for α $MgCl_2$ layers separated at a distance of 6.6 Å. The binding energy ($-\Delta E$) was found to be 23.7 kcal/mol for the (104) $MgCl_2$ layer and 28.5 kcal/mol for the (011) case. These values are less by 9.6 and 4.8 kcal/mol, respectively, than the binding energy obtained for the zip coordination of DIBP to (110) α $MgCl_2$ layers separated by 6.6 Å (33.3 kcal/mol). This validates the experimental and theoretical finding[14,29,35−37,45] that the (110) surface is the principal surface of consideration for the binding of DIBP to $MgCl_2$. The reason this is so is because of the decreased acidity of the magnesium atoms in the (104) and the (011) lateral cuts in comparison to the (110) due to the magnesium atoms being five-coordinated in the (104) and the (011) lateral cuts and being only four-coordinated in (110).

Overall, all the calculations have been done in this section by using the well-accepted[40,57−61] methodology of fixing all the support magnesium and chlorine atoms. While corroborations were seen between the calculated values and experiment, some discrepancies have also been observed and discussed above. The attempt in the next two sections using the Partially Relaxed and the Fully Relaxed Models is to try and address these observed discrepancies.

(B) Partially Relaxed Model. The $MgCl_2$ surface model that has been adopted for the calculations discussed in the previous sections keeps all the magnesium and chlorine atoms fixed. This, as mentioned in Computational Details, is the model that has been successfully employed in the past by computational groups to provide correct trends in the relative coordination energies.[40,57−61] However, as discussed in section A above, discrepancies were observed between the computational and experimental results for the 7.9 Å case. To investigate the causes of this discrepancy, the employed $MgCl_2$ model was modified by relaxing the surface magnesium and chlorine atoms. The zip coordination of one phthalate donor, DIBP, and one ester donor, *p*-isopropoxy ethyl benzoate, was studied, as before, at four interlayer distances: 5.9, 6.3, 6.6, and 7.9 Å. The optimized geometry of zip coordinated DIBP to the $MgCl_2$ layers is shown in Figure 7, while Table 3 show the ΔE values obtained for the coordination of DIBP and *p*-isopropoxy ethyl benzoate, respectively, to the α and β (110) $MgCl_2$ layers.

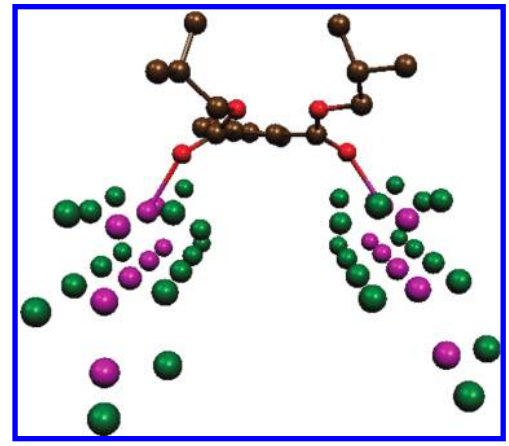

Figure 7. Optimized structure for the internal donor di-isobutyl phthalate on to the (110) α layers of $MgCl_2$ separated by 7.9 Å, and with the magnesium and chlorine atoms of the upper surfaces of the layers unfixed: the zip coordination is retained for this case; for the purpose of clarity, hydrogens are not shown.

TABLE 3: Values of ΔE Obtained for the Zip Coordination of the Internal Donor Di-isobutyl Phthalate and External Donor *p*-Iso-propoxy Ethyl Benzoate onto the (110) α and β layers of $MgCl_2$ with the Magnesium and Chlorine Atoms on the Upper Surface of the Layers Unfixed

distance (Å) between layers	ΔE (kcal/mol)			
	di-isobutyl phthalate		*p*-iso-propoxy ethyl benzoate	
	α	β	α	β
5.9	−40.8	−34.2	−20.2	−28.8
6.3	−35.1	−38.6	−32.4	−37.3
6.6	−35.7	−23.6	−33.5	−38.0
7.9	−31.3	−27.0	−30.5	−36.1

As Figure 7 indicates, DIBP is indeed seen to coordinate to the $MgCl_2$ surface at the large interlayer distance of 7.9 Å, unlike in the Fully Fixed Model where, as Figure 6 illustrated earlier, the donor loses the coordination to one of the two layers and only remains monocoordinated to the other $MgCl_2$ layer. The reason for this is that the coordinating magnesium atoms in the Fully Fixed Model are not allowed the freedom to move a little closer (7.55 Å) to coordinate to the sterically stretched oxygen atoms of the phthalate molecule, while the Partially Relaxed Model provides them that flexibility.

Table 3 indicates that while the obtained binding energies are about 1.0−2.0 kcal/mol greater than for the fully fixed $MgCl_2$ model for both the donors, the relative preferences of the phthalate and the alkoxy benzoate donors for the α and β $MgCl_2$ phases remains the same as before. This indicates that, for most of the range of interlayer distances, the Fully Fixed $MgCl_2$ model

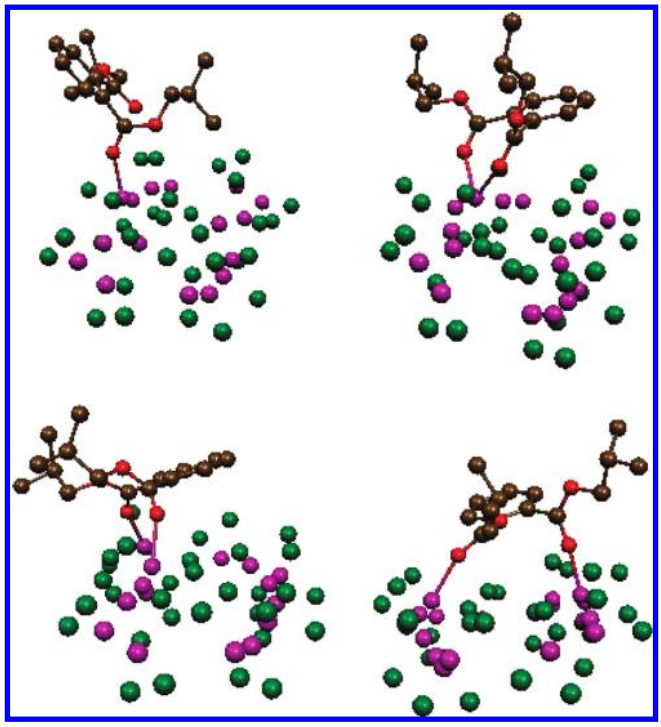

Figure 8. Shown in clockwise order, the optimized structures for the mono, chelate, zip, and bridge coordination of the internal donor diisobutyl phthalate onto the (110) α layers of $MgCl_2$: all the atoms are unfixed and allowed to move; for the purpose of clarity, hydrogens are not shown.

TABLE 4: Values of Δ*E* and Δ*G* Obtained for the Mono, Bridge, and Zip Coordination of the Internal Donor Di-isobutyl Phthalate onto the (110) α Layers of $MgCl_2$[a]

type of coordination	Δ*E* (kcal/mol)	Δ*G*[b] (kcal/mol)
mono	−32.5	−14.0
chelate	−26.8	−7.1
bridge	−38.1	−18.6
zip	−37.6	−19.4

[a] All the atoms are unfixed and allowed to move. [b] The distance between the magnesium atom to which the oxygen of the phthalate is coordinated, and the magnesium atom on the adjacent $MgCl_2$ surface.

can be expected to be reliable for providing relative trends in binding energies, but that at least a Partially Relaxed $MgCl_2$ model, such as the one employed and discussed here in this section, is necessary to provide complete agreement with experimental observations for the entire range where stability of $MgCl_2$ layers is observed in experimental studies.

(C) Fully Relaxed Model. Finally, it was also considered necessary to look at the different possible modes of coordination of the donor to the $MgCl_2$ surface when all the atoms were unfixed and allowed to move freely: the Fully Relaxed Model. Doing this (i) allows us to do frequency calculations and determine the free energies (−Δ*G*) of binding and also (ii) allows us to calculate C═O stretching frequencies to compare to experiment. Calculations were done looking at the four coordination modes, mono, chelate, bridge, and zip, possible for the DIBP donor onto the α (110) $MgCl_2$ surface. The optimized structures for the four cases are shown in Figure 8, while their Δ*E* and Δ*G* values of binding are collected together in Table 4. As the optimized structures collected in Figure 8 indicate, the layered structure of the (110) α $MgCl_2$ layers is lost in all the structures. This is the inevitable outcome when all the magnesium and the chlorine atoms in the adjacent layers are allowed full freedom of movement. However, the surface interactions between the donor and the magnesium and chlorine atoms, which is the primary focus of the investigation, are preserved.

It is interesting to note that the chelate coordination indeed does take place for the Fully Relaxed Model. The magnesium atom is seen to prefer accommodating the two oxygen atoms at the expense of weakening bonds to the adjacent chlorine atoms, something that the Fully Fixed Model would not, of course, allow. Also, a look at the Δ*E* values in Table 4 indicates that the monocoordination mode of binding is underestimated by the Fully Fixed Model; for the same reason, the coordinating magnesium atoms prefer to weaken their chlorine bonds to bind to the oxygen atoms.

As expected, the Δ*G* values are considerably less negative, by about 18.0−20.0 kcal/mol, for the four cases, because of the entropic cost of bringing the $MgCl_2$ layers together. Nevertheless, all the Δ*G* values are negative, ranging from −7.1 kcal/mol for the chelate coordination mode to −19.4 kcal/mol for the zip coordination mode (see Table 4), indicating the feasibility of the binding of DIBP to the $MgCl_2$ surface through all the four coordination modes.

Comparing the Fully Relaxed Model to the Fully Fixed and the Partially Relaxed Models, it is noted that the relative electronic binding energies (−Δ*E*) follow the same trend for the mono, bridge, and zip coordination modes as had been seen before for the previous two models, with the monocoordination mode being the least facile and the bridge coordination the most favored of the three. However, it is interesting to note that the trend is changed slightly when comparing the Δ*G* values for binding. It is seen that the zip coordination mode becomes the most favored when entropic effects are taken into account.

Doing free energy calculations with the Fully Relaxed Model also allowed us to calculate the (>C═O) stretching frequencies. For the free DIBP molecule, two (>C═O) stretching frequencies at 1740.6 and 1707.5 cm^{-1} were observed, while the (>C═O) stretching frequencies were reduced considerably (i) for the monocoordinated DIBP case, to 1687.4 cm^{-1} (for the unbound >C═O group) and to 1642.1 cm^{-1} (the bound >C═O) group, (ii) for the chelate coordinated DIBP case, to 1626.9 and 1664.7 cm^{-1}, (iii) for the bridge coordinated case, to 1637.7 and 1621.4 cm^{-1}, and (iv) for the zip-coordinated case, to 1665.0 and 1655.5 cm^{-1}. This computationally determined reduction in the (>C═O) stretching frequency provides an explanation for the experimentally observed wide range in the (>C═O) stretching frequency between 1600−1700 cm^{-1} for the $MgCl_2$/$TiCl_4$/DIBP system.[19,45,63,64]

(D) Insertion Studies. Using a pair of succinate donors, Correa et al.[40] have studied the effect of bridge coordination on the regio- and stereoselectivity of propylene insertion on a Δ coordinated titanium center. If, as our investigations indicate, the zip coordination is a competitive mode of coordination of the donors on to the $MgCl_2$ surface, it is important to determine the effect of zip-coordinating donors on the regio and stereoselectivity of a titanium center. This is what has been attempted and is discussed in this section. Like Correa et al.,[40] we have fixed the configuration of the titanium complex as Δ, studied propylene insertion into the Ti-*i*Bu bond, and also followed the same method for determining the approximate transition state for the insertion as they had adopted (see also Computational Details). Also, like Correa et al.,[40] we have employed the Partially Relaxed Model for our calculations and investigated all the four possible modes of insertion: two primary (1,2-insertion: *si* and *re* face) and two secondary (2,1-insertion:

TABLE 5: Formation of the π Complex (ΔE_π[a]) from the Separated Reactants, the Ti(III) Catalyst Center on the Zip-Coordinated $MgCl_2$ Surface and the Propylene, and the Subsequent Barrier to Insertion for the Propylene into the Titanium-Alkyl Bond[b]

type of insertion	ΔE_π (kcal/mol)	$\Delta E_{TS}{}^1$ (kcal/mol)	$\Delta E_{TS}{}^2$ (kcal/mol)	relative barriers (kcal/mol)
Primary Insertion (1,2)				
si face	−7.6	10.7	3.1	0.0
re face	−8.6	12.7	4.1	1.0
Secondary Insertion (2,1)				
si face	−9.4	16.2	6.8	3.7
re face	not favorable	not favorable	not favorable	not favorable

[a] Values of ΔE in kcal/mol. [b] $\Delta E_{TS}{}^1$ is calculated with respect to the π complex and $\Delta E_{TS}{}^2$ is calculated with respect to the separated reactants.

si and the *re* face). The α $MgCl_2$ (110) surface has been considered for the studies, with the distance between the layers kept at 5.9 Å. One notable additional set of calculations that we have done has been to also determine the energy of formation of the π-complex before insertion. The results of our calculations are collected together in Table 5. "ΔE_π" in Table 5 denotes the energy gained due to complexation of the propylene to the titanium center, while $\Delta E_{TS}{}^1$ refers to the difference in energy between the transition state and the π complex. $\Delta E_{TS}{}^2$ refers to the overall barrier of the reaction, calculated by subtracting the energy of the transition state from the energies of the separated reactants: the zip-coordinated titanium complex and the propylene. Finally, the last column indicates the relative insertion barriers for the four cases, with the lowest insertion barrier (that of the *si*-primary insertion) taken as 0.0 kcal/mol.

As Correa et al. had shown, in the absence of any donors, the insertion of propylene into a Ti-*i*Bu bond shows almost no regio- or stereoselective preference,[40] while the presence of flanking bridge coordinating donors was found to have a significant effect on the steroselectivity and a marginal effect on the regio-selectivity.[40] As Table 5 indicates, our results show that the presence of flanking zip-coordinating donors leads to the primary insertion still being the preferred mode of insertion for the propylene into the Ti-*i*Bu. Interestingly, however, contrary to the bridge coordinated case, zip coordination makes propylene insertion highly regioselective and only moderately stereoselective. Like in the bridge coordinating case, our results indicate that the *si*-primary insertion mode is still the favored mode of insertion, but unlike the bridge coordinating case, the primary insertion at the *re*-face is only slightly less favorable (higher by 1.0 kcal/mol). On the other hand, the secondary insertion is highly unfavorable; the results indicate that *re*-secondary insertion is completely disfavored, while *si*-secondary insertion is disfavored by 3.7 kcal/mol relative to the *si*-primary insertion. The reason for this is the steric strain produced in the system by the proximity of the methyl group on the 2,1-coordinated propylene with the zip-coordinated DIBP donor. As the optimized secondary π complex structures in Figure 9 illustrate, the isobutyl group on the DIBP donor is too close to the propylene CH_3 group. Indeed, all attempts to optimize the *re*-secondary π complex led to the propylene moiety swinging away to recoordinate to the titanium center as the *si*-secondary π complex, which also eventually shows a high barrier to insertion (see Table 5), thus, showing that zip coordination of the donors completely eliminates the *re*-secondary mode of insertion of propylene and reduces the possibility of the *si*-secondary mode of coordination. The steric effect is less pronounced for the primary insertions, which is why *si*-primary is only slightly preferred with respect to the *re*-primary mode of insertion.

Overall, the results indicate that zip coordination of the donors can not only have an effect on the stability of the $MgCl_2$ layers (as seen in the previous sections), but that it can also lead to modulation of the properties of the polymer produced during the Ziegler−Natta polymerization, conferring regioselectivity (to a considerable extent) and stereoselectivity (to a lesser extent) to a titanium center.

(E) Potential External Donor Candidates for Internal Donor DIBP. It is well-known that the addition of a base as an "external" donor can have a significant impact on the isotacticity of the final polymer product.[29−32] It is believed that the role of the external donor includes replacing the internal donor that has been displaced from the $MgCl_2$ surface.[62] Because our calculations have underlined the significance of zip coordination of the internal donor to the $MgCl_2$ surface, both in terms of stabilizing the $MgCl_2$ layers as well as in providing regio- and stereoselectivity to the titanium center, we decided to also look at other bidentate donor molecules that could potentially zip coordinate and replace a DIBP molecule on the $MgCl_2$ surface, that is, act as an external donor. An example of this is shown in Figure 10, a 1,3-diether molecule, 3,3-bis(methoxymethyl)-2,4-dimethylpentane, that is zip-coordinated to $MgCl_2$ alongside a DIBP molecule (the figure shows the optimized structure).

A list of nine such potential bidentate external donors has been considered here and their zip-coordinated structures optimized alongside DIBP. The structures of these nine bidentate donor molecules are shown in Figure 11. Some of the donors considered are ones that are commonly used in industry such as benzoates, alkoxy silanes, succinates, and diethers. In addition, some potential new donors that have not been used to date as donors have also been investigated, molecules such as a cyano-benzoate and a pyridine ester. Such donors have been

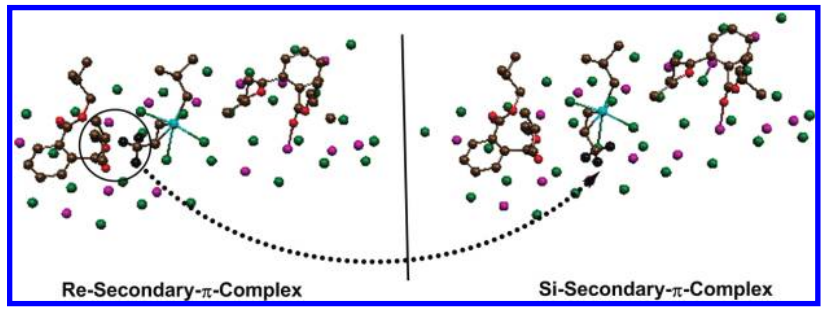

Figure 9. Steric effect of the zip-coordinated DIBP donors on the secondary insertion: during the optimization of the *re*-secondary π complex, the close proximity of the isobutyl group of the phthalate forces the CH_3 group to rotate away to the *si*-secondary π complex position; all other hydrogens are not shown for purposes of clarity (note: the atom in blue is titanium, flanked by zip coordinating DIBP donors).

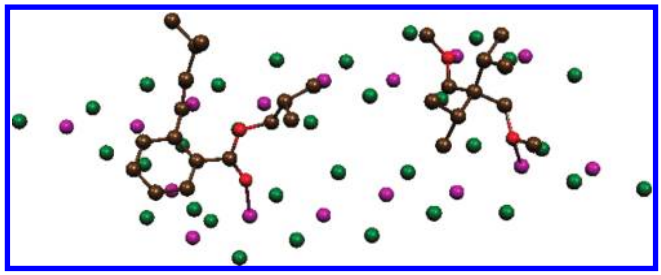

Figure 10. Replacement of one zip-coordinating DIBP donor with an "external" donor, a 1,3-diether, that also zip-coordinates to the $MgCl_2$ surface; the optimized geometry is shown.

indicated with an asterisk in Table 6. The binding energy of the external donor to the $MgCl_2$ surface, ΔE in Table 6, has been determined by subtracting the energy of the two reactants, (i) the $MgCl_2$ layers containing a single, zip-coordinated DIBP molecule and (ii) the external donor from the product: the $MgCl_2$ layers containing both the DIBP and the external donor zip-coordinated to the surface. As had been done for the insertion studies in section (D) above, the Partially Relaxed Model has been considered for the α $MgCl_2$ (110) surface, with the distance between the layers kept at 5.9 Å.

Table 6 shows the values of ΔE calculated for the nine cases, along with that of DIBP as the tenth case, the molecule that would be replaced by the external donor. Also indicated in Table 6 is the relative stability conferred on the $MgCl_2$ surface by the external donor when it replaces DIBP, the relative value of the ΔE when the ΔE for the DIBP case is taken as 0.0 kcal/mol (see Table 6).

As the numbers in Table 6 indicate, some of the donors, the ones lying above DIBP in the table, have positive relative energy values compared to DIBP and would therefore be predicted to not be good external donors when DIBP is the internal donor. However, three of the donors considered, the pyridine ester, diisobutyl pyridine-2,6-dicarboxylate (not used to date), the diacetoxy silane, diphenylsilanediyl diacetate, and especially the 1,3-diether-3,3-bis(methoxymethyl)-2,4-dimethylpentane, would be predicted to serve as excellent substitutes to DIBP, because their energies of binding to the $MgCl_2$ surface are greater than that of DIBP. Indeed, the strong zip-coordinating affinity of the 1,3-diether donor molecule to the $MgCl_2$ surface may help explain why such 1,3-diethers, used as internal donors with no requirement for an external donor, have become most successful in providing stereo- and regioselectivity to polymers obtained from Ziegler−Natta catalyst systems.[65]

TABLE 6: Values of ΔE in kcal/mol for (i) the Zip Coordination Binding of a Second, "External" Donor to an $MgCl_2$ Surface Already Possessing One Zip-Coordinated DIBP Molecule and (ii) the Energies of Binding of the External Donor with Respect to DIBP[a]

donor	binding energy (kcal/mol)	relative energy (kcal/mol)
3,3′-dimethyl-4,4′-bipyridine	−9.9	+23.7
dicyclopentyl-dimethoxysilane	−15.9	+17.7
ethyl 4-cyanobenzoate*	−25.4	+8.2
1,2-bis(diphenylphosphino)ethane*	−27.7	+5.9
ethyl 4-*tert*-butoxybenzoate	−28.7	+4.9
diethyl 2,3-diisopropylsuccinate	−32.4	+1.2
DIBP	−33.6	0.0
diisobutyl pyridine-2,6-dicarboxylate*	−35.2	−1.6
diphenylsilanediyl diacetate	−42.8	−9.2
3,3-bis(methoxymethyl)-2,4-dimethylpentane	−48.8	−15.2

[a] The asterisk on some of the donors indicates that they have not been employed previously in industry.

Conclusions

Modern day Ziegler−Natta catalyst systems for alkene polymerization employ different combinations of internal and external donors to obtain high productivity and stereoselectivity in olefin-based polymers. The computational investigations discussed here, employing density functional theory, are an attempt to expand on the current understanding of the role of the internal and external donors, especially on their influence in stabilizing the $MgCl_2$ support and on the regio- and stereoselectivity of the catalyst center. For this purpose, density functional theory calculations have been done to study the coordination of different phthalate and alkoxy benzoate donors to α and β (110) lateral cuts of $MgCl_2$ (calculations with β phase $MgCl_2$ being done for the first time). Three different models have been employed to represent the $MgCl_2$ support: the Fully Fixed Model, where all the atoms of the $MgCl_2$ support have been kept fixed, the Partially Relaxed Model, where the atoms

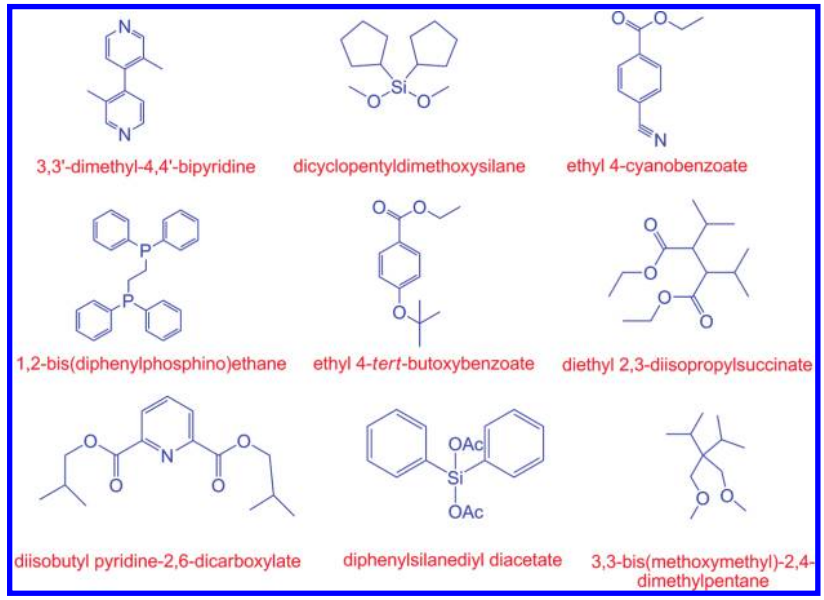

Figure 11. Nine external donors that have been considered as substitutes for DIBP for zip coordination to the $MgCl_2$ surface.

in the top layer of the lateral cuts of $MgCl_2$ were kept free, and the Fully Relaxed Model, where all the atoms in the $MgCl_2$ support were allowed to move. The donor atoms have been kept unfixed in all the three models. Two different phthalate donors, di-isobutyl and diethyl phthalate (DIBP and DEP, respectively), and three different alkoxy benzoate donors, *p*-isopropoxy, *p*-ethoxy, and *p*-*tert*-butoxy benzoate, have been considered as representative internal and external donors, respectively. Of the four possible coordination modes of the donors, the mono, chelate, bridge, and zip coordination modes (see Figure 2), emphasis was placed on investigating the zip coordination of the donors to the $MgCl_2$ lateral cuts, to explain the experimentally observed[45] stability of the $MgCl_2$ microcrystals for interlayer distances ranging from 5.9−7.9 Å.

The results indicate that the Fully Fixed Model provides a reliable means of determining the trends in donor binding to the α and β phases of $MgCl_2$, with only a few discrepancies noticed between the computed results and experiment, which are corrected by the use of the Partially Relaxed and the Fully Relaxed Models. The obtained results provide a basis for explaining why certain donor combinations are experimentally very effective in Ziegler−Natta polymerization systems. Also, insertion studies done at the octahedrally chiral titanium center indicate that the presence of flanking zip-coordinated DIBP donors confers regioselectivity (to a great extent) and stereoselectivity (to a lesser extent) to the catalyst center, with the *si*-primary mode being the preferred route to insertion. Finally, the study of possible replacements to a zip-coordinated DIBP at the $MgCl_2$ surface indicates that 1,3-diethers are excellent zip-coordinating donors, which may help explain the high isotacticity obtained when they are employed in industry. The calculations also predict that pyridine esters may be potentially good donors for the Ziegler−Natta catalyst system.

Overall, the current investigation has expanded on the role of internal and external donors employed in Ziegler−Natta catalyst systems and shown that a significant role of the donors is the stabilization of the α (ccp) or the β (hcp) phases of $MgCl_2$ and also that zip coordination of the donors leads to significant improvement in the regioselectivity of the catalyst center.

Acknowledgment. K.V. and D.I. wish to thank the Centre of Excellence in Scientific Computing (COESC) at the National Chemical Laboratory (NCL), Pune, for providing computational facilities.

Supporting Information Available: The tabulated comparison of results obtained with the Partially Relaxed and the Fully Fixed Models with previously published periodic DFT calculations is provided. Also provided are the Cartesian coordinates for all the optimized structures discussed in the text. This material is available free of charge via the Internet at http://pubs.acs.org.

References and Notes

(1) Galli, P.; Vecellio, G. *J. Polym. Sci., Part A: Polym. Chem.* **2004**, *42*, 396–415.
(2) Corradini, P. *J. Polym. Sci., Part A: Polym. Chem.* **2004**, *42*, 391–395.
(3) Chum, P. S.; Swogger, K. W. *Prog. Polym. Sci.* **2008**, *33*, 797–819.
(4) Corradini, P.; Guerra, G.; Cavallo, L. *Acc. Chem. Res.* **2004**, *37*, 231–241.
(5) Galli, P. *Macromol. Symp.* **1995**, *89*, 11.
(6) Gupta, V. K. *J. Polym. Mater.* **1999**, *16*, 97.
(7) Chadwick, J. C. *Macromol. Symp.* **2001**, *173*, 21.
(8) Cheng, H. N. *Macromol. Theory Simul.* **1993**, *2*, 901.
(9) Cavallo, L.; Guerra, G.; Corradini, P. *J. Am. Chem. Soc.* **1998**, *120*, 2428.
(10) Busico, V.; Cipullo, R.; Monaco, G.; Vacatello, M.; Segre, A. L. *Macromolecules* **1997**, *30*, 6251.
(11) Busico, V.; Cipullo, R. *Prog. Polym. Sci.* **2001**, *26*, 443.
(12) Chadwick, J. C.; van der Burgt, F. P. T. J.; Rastogi, S.; Busico, V.; Cipullo, R.; Talarico, G.; Heere, J. J. R. *Macromolecules* **2004**, *37*, 9722.
(13) Kim, S. H.; Somorjai, G. A. *J. Phys. Chem. B* **2001**, *105*, 3922.
(14) Mori, H.; Sawada, M.; Higuchi, T.; Hasebe, K.; Otsuka, N.; Terano, M. *Macromol. Rapid Commun.* **1999**, *20*, 245–250.
(15) Andoni, A.; Chadwick, J. C.; Milani, S.; Niemantsverdriet, H. J. W.; Thüne, P. C. *J. Catal.* **2007**, *247*, 129–136.
(16) Andoni, A.; Chadwick, J. C.; Niemantsverdriet, H. J. W.; Thüne, P. C. *Macromol. Rapid Commun.* **2007**, *28*, 1466–1471.
(17) Andoni, A.; Chadwick, J. C.; Niemantsverdriet, H. J. W.; Thüne, P. C. *Macromol. Symp.* **2007**, *260*, 140–146.
(18) Andoni, A.; Chadwick, J. C.; Niemantsverdriet, H. J. W.; Thüne, P. C. *J. Catal.* **2008**, *257*, 81–86.
(19) Potapov, A. G.; Bukatov, G. D.; Zakharov, V. A. *J. Mol. Catal. A: Chem.* **2006**, *246*, 248–254.
(20) Busico, V.; Causa, M.; Cipullo, R.; Credendino, R.; Cutillo, F.; Friederichs, N.; Lamanna, R.; Segre, A.; Castelli, V. V. A. *J. Phys. Chem. C* **2008**, *112*, 1081–1089.
(21) Monaco, G.; Toto, M.; Guerra, G.; Corradini, P.; Cavallo, L. *J. Phys. Chem. C* **2000**, *33*, 8953–8962.
(22) Giannini, U. *Makromol. Chem. Suppl.* **1981**, *5*, 216.
(23) Noto, V. D.; Bresadola, S. *Macromol. Chem. Phys.* **1996**, *197*, 3827–3835.
(24) Noto, V. D.; Fregonese, D.; Marigo, A.; Bresadola, S. *Macromol. Chem. Phys.* **1998**, *199*, 633–640.
(25) Vittadello, M.; Stallworth, P. E.; Alamgir, F. M.; Suarez, S.; Abbrent, S.; Drain, C. M.; Noto, V. D.; Greenbaum, S. G. *Inorg. Chim. Acta* **2006**, *359*, 2513–2518.
(26) Hu, Y.; Chien, J. C. W. *J. Polym. Sci., Part A: Polym. Chem.* **1988**, *26*, 2003–2018.
(27) Chein, J. C. W.; Wu, J. C.; Kuo, C. I. *J. Polym. Sci., Part A: Polym. Chem.* **1983**, *21*, 737–750.
(28) Marigo, A.; Marega, C.; Zannetti, R.; Morini, G.; Ferrera, G. *Eur. Polym. J.* **2000**, *36*, 1921–1926.
(29) Taniike, T.; Terano, M. *Macromol. Rapid Commun.* **2008**, *29*, 1472–1476.
(30) Boero, M.; Parrinello, M.; Hüffer, S.; Weiss, H. *J. Am. Chem. Soc.* **2000**, *122*, 501–509.
(31) Brambilla, L.; Zerbi, G.; Piemontesi, F.; Nascetti, S.; Morini, G. *J. Mol. Catal. A: Chem.* **2007**, *263*, 103–111.
(32) Ribour, D.; Monteil, V.; Spitz, R. *J. Polym. Sci., Part A: Polym. Chem.* **2008**, *46*, 5461–5470.
(33) Scordamaglia, R.; Barino, L. *Macromol. Theory Simul.* **1998**, *7*, 399–405.
(34) Toto, M.; Morini, G.; Guerra, G.; Corradini, P.; Cavallo, L. *Macromolecules* **2000**, *33*, 1134–1140.
(35) Seth, M.; Margl, P. M.; Ziegler, T. *Macromolecules* **2002**, *35*, 7815–7829.
(36) (a) Seth, M.; Margl, P. M.; Ziegler, T. *Macromolecules* **2003**, *36*, 6613–6623. (b) Flisak, Z. *Macromolecules* **2008**, *41*, 6920–6924.
(37) Seth, M.; Margl, P. M.; Ziegler, T. *Macromolecules* **2004**, *37*, 9191–9200.
(38) Boero, M.; Parrinello, M.; Weiss, H.; Hüffer, S. *J. Phys. Chem. A* **2001**, *105*, 5096–5105.
(39) Trubitsyn, D. A.; Zakharov, V. A.; Zakharov, I. I. *J. Mol. Catal. A: Chem.* **2007**, *270*, 164–170.
(40) Correa, A.; Piemontesi, F.; Morini, G.; Cavallo, L. *Macromolecules* **2007**, *40*, 9181–9189.
(41) Kissin, Y. V.; Chadwick, J. C.; Mingozzi, I.; Morini, G. *Macromol. Chem. Phys.* **2006**, *207*, 1344–1350.
(42) Chadwick, J. C.; Morini, G.; Balbontin, G.; Camurati, I.; Heere, J. J. R.; Mingozzi, I.; Testoni, F. *Macromol. Chem. Phys.* **2001**, *202*, 1995–2002.
(43) Albizzati, E.; Giannini, U.; Collina, G.; Noristi, L.; Resconi, L. Catalysts and Polymerizations. In *Polymerization Handbook*; Moore, E. P., Ed.; Hanser-Gardner Publications: Cincinnati, OH, 1996; Chapter 2.
(44) Lieberman, R.; Stewart, C. Propylene Polymers. In *Encyclopedia of Polymer Science and Technology*; Mark, H. F., Ed.; John Wiley and Sons, Inc.: New York, 2004; vol. *11*, p 310.
(45) Singh, G.; Kaur, S.; Makwana, U.; Patankar, R. B.; Gupta, V. K. *Macromol. Chem. Phys.* **2009**, *210*, 69–76.
(46) Ahlrichs, R.; Bär, M.; Baron, H.-P.; Bauernschmitt, R.; Böcker, S.; Ehrig, M.; Eichkorn, K.; Elliott, S.; Furche, F.; Haase, F.; Häser, M.; Horn, H.; Huber, C.; Huniar, U.; Kattannek, M.; Kölmel, C.; Kollwitz, M.; May, K.; Ochsenfeld, C.; Öhm, H.; Schäfer, A.; Schneider, U.; Treutler, O.; von Arnim, M.; Weigend, F.; Weis, P.; Weiss, H. *Turbomole*, version 5.3; Universität Karlsruhe: Karlruhe, Germany, 2000.

(47) Schäfer, A.; Huber, C.; Ahlrichs, R. *J. Chem. Phys.* **1994**, *100*, 5829.
(48) Schäfer, A.; Horn, H.; Ahlrichs, R. *J. Chem. Phys.* **1992**, *97*, 2571.
(49) Andrae, D.; Haeussermann, U.; Dolg, M.; Stoll, H.; Preuss, H. *Theor. Chim. Acta* **1990**, *77*, 123.
(50) Perdew, J. P.; Wang, Y. *Phys. Rev. B: Condens. Matter* **1992**, *45*, 13244–13249.
(51) Perdew, J. P.; Burke, K.; Ernzerhof, M. *Phys. Rev. Lett.* **1996**, *77*, 3865–3868.
(52) Schäfer, A.; Horn, H.; Ahlrichs, R. *J. Chem. Phys.* **1992**, *97*, 2571–2577.
(53) (a) Eichkorn, K.; Treutler, O.; Öhm, H.; Häser, M.; Ahlrichs, R. *Chem. Phys. Lett.* **1995**, *240*, 283.
(54) Sierka, M.; Hogekamp, A.; Ahlrichs, R. *J. Chem. Phys.* **2003**, *118*, 9136–9148.
(55) Pennington, W. T. *J. Appl. Crystallogr.* **1999**, *32*, 1028–1029.
(56) Macrae, C. F.; Bruno, J.; Chisholm, J. A.; Edgington, P. R.; McCabe, P.; Pidcock, E.; Rodriguez-Monge, L.; Taylor, R.; van de Streek, J.; Wood, P. A. *J. Appl. Crystallogr.* **2008**, *41*, 466–470.
(57) Puhakka, E.; Pakkanen, T. T.; Pakkanen, T. A. *Surf. Sci.* **1995**, *334*, 289–294.
(58) Puhakka, E.; Pakkanen, T. T.; Pakkanen, T. A. *J. Mol. Catal. A: Chem.* **1997**, *120*, 143–147.
(59) Puhakka, E.; Pakkanen, T. T.; Pakkanen, T. A. *J. Phys. Chem. A* **1997**, *101*, 6063–6068.
(60) Puhakka, E.; Pakkanen, T. T.; Pakkanen, T. A. *J. Mol. Catal. A: Chem.* **1997**, *123*, 171–178.
(61) Puhakka, E.; Pakkanen, T. T.; Pakkanen, T. A.; Iiskola, E. *J. Organomet. Chem.* **1996**, *511*, 19–27.
(62) Taniike, T.; Terano, M. *Macromol. Symp.* **2007**, *260*, 98.
(63) Kissin, Y. V.; Liu, X.; Pollick, D. J.; Brungard, N. L.; Chang, M. *J. Mol. Catal. A: Chem.* **2008**, *287*, 44–51.
(64) Stukalov, D. V.; Zakharov, V. A.; Potapov, A. G.; Bukatov, G. D. *J. Catal.* **2009**, *266*, 39–49.
(65) Albizatti, E.; Giannini, U.; Morini, G.; Galimberti, M.; Barino, L.; Scordamaglia, R. *Macromol. Symp.* **1995**, *89*, 73.
(66) Woo, T. K.; Margl, P. M.; Blöchl, P. E.; Ziegler, T. *J. Am. Chem. Soc.* **1996**, *118*, 13021.
(67) Tomasi, S.; Weiss, H.; Ziegler, T. *Organometallics* **2006**, *25*, 3619.

JP106673B